

UC San Diego

UC San Diego Previously Published Works

Title

Molecular stripping in the NF- κ B/I κ B/DNA genetic regulatory network

Permalink

<https://escholarship.org/uc/item/41k7w33s>

Journal

Proceedings of the National Academy of Sciences of the United States of America,
113(1)

ISSN

0027-8424

Authors

Potoyan, Davit A
Zheng, Weihua
Komives, Elizabeth A
et al.

Publication Date

2016-01-05

DOI

10.1073/pnas.1520483112

Peer reviewed

Molecular stripping in the *NF-κB/IκB/DNA* genetic regulatory network

Davit A. Potoyan^a, Weihua Zheng^a, Elizabeth A. Komives^b, and Peter G. Wolynes^{a,1}

^aCenter for Theoretical Biological Physics and Department of Chemistry, Rice University, Houston, TX 77005; and ^bDepartment of Chemistry and Biochemistry, University of California, San Diego, La Jolla, CA 92093

Contributed by Peter G. Wolynes, November 16, 2015 (sent for review October 16, 2015; reviewed by Yaakov Levy and John J. Portman)

Genetic switches based on the *NF-κB/IκB/DNA* system are master regulators of an array of cellular responses. Recent kinetic experiments have shown that *IκB* can actively remove *NF-κB* bound to its genetic sites via a process called “molecular stripping.” This allows the *NF-κB/IκB/DNA* switch to function under kinetic control rather than the thermodynamic control contemplated in the traditional models of gene switches. Using molecular dynamics simulations of coarse-grained predictive energy landscape models for the constituent proteins by themselves and interacting with the DNA we explore the functional motions of the transcription factor *NF-κB* and its various binary and ternary complexes with DNA and the inhibitor *IκB*. These studies show that the function of the *NF-κB/IκB/DNA* genetic switch is realized via an allosteric mechanism. Molecular stripping occurs through the activation of a domain twist mode by the binding of *IκB* that occurs through conformational selection. Free energy calculations for DNA binding show that the binding of *IκB* not only results in a significant decrease of the affinity of the transcription factor for the DNA but also kinetically speeds DNA release. Projections of the free energy onto various reaction coordinates reveal the structural details of the stripping pathways.

protein–DNA interaction | allostery | genetic switch | molecular dynamics | systems biology

The binding and release of protein transcription factors from DNA are fundamental molecular processes by which genes are regulated in the cell. The pioneering studies of Jacob, Monod, Ptashne, and Gilbert explained how these two processes, seeming inverses of each other, while being maintained in local chemical equilibrium, could still lead to robust genetic switches by coupling to protein synthesis and degradation, which are kinetically controlled far from equilibrium processes (1–4). This classic picture, with the law of mass action at its core (5, 6), suggests that understanding the molecular mechanism of the binding and release of transcription factors is of secondary interest compared with understanding the thermodynamics of protein–DNA recognition. The recent discovery of protein-induced release of a DNA-bound transcription factor in the *NF-κB/IκB/DNA* genetic switch changes this picture (7). The induced process, called “molecular stripping,” opens up the possibility of molecular kinetic control of binding and release, thus overturning the classic paradigm based only on thermodynamic control. In this paper, we use molecular dynamics simulations of coarse-grained but predictive energy landscape models of the proteins along with their interacting DNA to explore first how the *NF-κB* transcription factor binds individually both to DNA and to its inhibitor *IκB* and then to study how an approaching *IκB* can strip the *NF-κB* from a DNA molecule to which it has already been bound, by forming an intermediate ternary complex. These simulations show that each of the binary binding events involves conformational selection of different *NF-κB* global conformations. Molecular stripping then occurs that is induced by forming the ternary complex. Stripping involves changes in the patterns of local frustration in the proteins and an interchange of electrostatic interactions between the

protein–protein and the protein–DNA partners. The simulations highlight the breaking of symmetry in the *NF-κB* heterodimer complex with *IκB* as well as the important role of the PEST sequence [protein sequence rich in proline (P), glutamic acid (E), serine (S), and threonine (T)] of *IκB* in the stripping.

Systems Biology of *NF-κB/IκB/DNA*

The transcription factor *NF-κB* is central to the regulation of inflammatory responses, immune responses to infections, and programmed cell death. *NF-κB* is a collective name for a family of homo- and heterodimeric proteins that serve as a bridge from the extracellular signals to gene expression (8). The *NF-κB* heterodimer p50p65 is the most abundant form, although other forms are also present in the cell. *NF-κB* is activated by a diverse set of extracellular stimuli that through an enzyme cascade mark the *IκB* moiety for degradation, subsequently freeing *NF-κB* from its inhibited complex. In its active, unbound form *NF-κB* translocates to the nucleus, thereby initiating the transcription of hundreds of genes. Owing to its wide range of influence *NF-κB* is considered a “master regulator switch” (9). Among the target genes of *NF-κB* is its own inhibitor *IκBα*, which we will refer to simply as *IκB*. Targeting *IκB* synthesis results in a negative feedback loop that governs the nuclear concentration of active *NF-κB*, leading to pulses of activation and inactivation (10, 11). *IκB* strips the *NF-κB* off from its DNA targets and masks the nuclear localization signal of the *NF-κB* (7). The resulting tightly bound *NF-κB*–*IκB* complex (12) is thus prevented from reentering the nucleus (13, 14), thereby terminating all of the associated genetic activities of *NF-κB* to restore the cellular resting state (Fig. 1A).

The most complete mathematical models of *NF-κB* signaling have assumed fast local equilibria for *NF-κB* binding to the DNA (15, 16). Recent in vitro kinetic measurements of *IκB* binding to the complex of *NF-κB* with DNA challenge this equilibrium view. *NF-κB* dissociates from DNA in an *IκB*

Significance

The classic models of genetic switches are based on thermodynamic control via binding affinities. Complex nonequilibrium eukaryotic gene networks with many targets such as the *NF-κB/IκB/DNA* system challenge this picture. Waiting for unbinding from the numerous *NF-κB* binding sites takes time that would allow wasteful overexpression of many genes. Active molecular stripping of *NF-κB* from the DNA by *IκB* solves the timescale problem raised in the classic picture based on thermodynamics alone.

Author contributions: D.A.P., W.Z., E.A.K., and P.G.W. designed research; D.A.P. and W.Z. performed research; D.A.P. and W.Z. contributed new reagents/analytic tools; D.A.P., W.Z., E.A.K., and P.G.W. analyzed data; and D.A.P., E.A.K., and P.G.W. wrote the paper.

Reviewers: Y.L., Weizmann Institute of Science; and J.J.P., Kent State University.

The authors declare no conflict of interest.

¹To whom correspondence should be addressed. Email: pwolynes@rice.edu.

This article contains supporting information online at www.pnas.org/lookup/suppl/doi:10.1073/pnas.1520483112/-DCSupplemental.

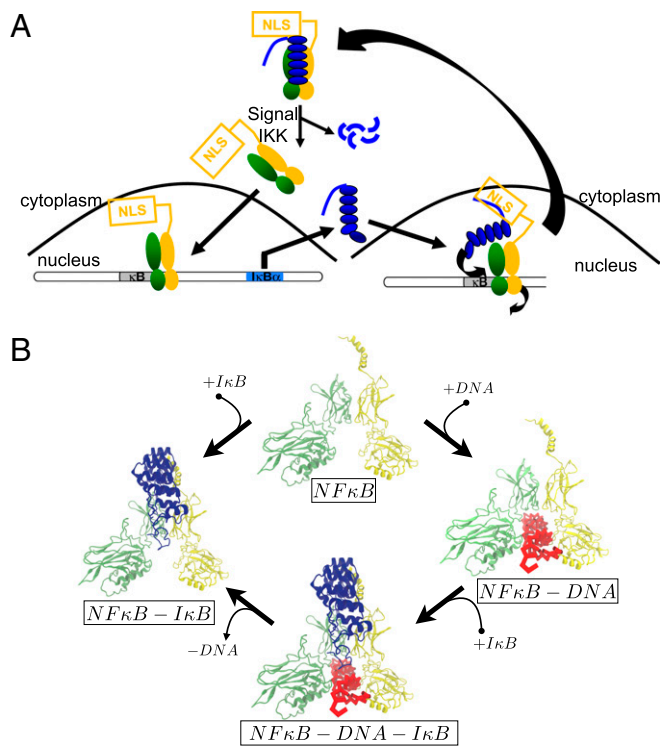


Fig. 1. (A) Schematic systems biology view of $NF-\kappa B$ regulation by its inhibitor $I\kappa B$. Shown are the key steps of a negative feedback cycle that includes the $NF-\kappa B$ activation by external stimuli (IKK), followed by NLS-mediated translocation to the nucleus, DNA binding, $I\kappa B$ synthesis, and molecular stripping of $NF-\kappa B$ by $I\kappa B$. (B) Diagram showing the predicted structures used in the simulations. The names of complexes are shown at the bottom of the structures. Arrows indicate the thermodynamically favored directions for interconversion between the complexes given sufficient concentrations of the $I\kappa B$ and the DNA binding sites.

concentration-dependent manner (7, 17). Including this enhancement in models requires going beyond the purely equilibrium picture that envisions fast dissociation/association and that ignores competing binding at other gene sites. A revised systems biology scheme showing the central role of molecular stripping is described in Fig. 1A. In vivo there are several thousand κB binding sites (18); thus, if dissociation from these target and decoy sites would not be fast enough there would be wasteful overexpression of genes. Rapid molecular stripping of $NF-\kappa B$ from its DNA results in efficient down-regulation of the $NF-\kappa B$ targets, ensuring the optimal expenditure of cellular resources. Our simulations demonstrate a feasible mechanism for this molecular stripping reaction.

Structures, Dynamics, and Thermodynamics

Structures of the p50p65 heterodimer of $NF-\kappa B$ bound with the DNA and with its inhibitor $I\kappa B$ have already been resolved with X-ray crystallography (14, 19, 20). Unfortunately, each of the available structures lacks at least one mechanistically crucial part of the $NF-\kappa B$ molecule. The structure of $NF-\kappa B - DNA$ (PDB ID code 1LE5) by Berkowitz et al. (19) lacks the crucial nuclear localization signal (NLS), and the entire p50 N-terminal binding domain is missing from the two existing crystal structures (14, 20) for $NF-\kappa B - I\kappa B$ (PDB ID codes 1IKN and 1NFI). To understand the binding and stripping mechanisms, more complete structures are needed. To construct these structures (Fig. 1B) we carried out simulations with a coarse-grained protein–DNA force field. We added the missing molecular fragments and regenerated the full structures of the various complexes by using

the Associative memory, Water mediated, Structure and Energy Model (AWSEM) for the interactions within and among the proteins (21) and the Three Sites Per Nucleotide (3SPN) model for the DNA (22, 23). DNA and protein are coupled through steric exclusion and electrostatics modeled at the mean field level. AWSEM is a coarse-grained predictive model based on the energy landscape formulation of protein folding theory (24). It accounts explicitly for physically motivated interactions such as hydrogen bonding and solvent interactions to model tertiary structure relationships and incorporates “evolutionary forces” via bioinformatic terms that act locally in sequence. Both kinds of interactions effectively sculpt the landscapes of naturally occurring proteins to be highly funneled toward the native state. AWSEM has proved successful in predicting structures of both protein monomers (21) and dimers (25). The 3SPN force field is a coarse-grained model for the DNA that also includes physically motivated terms, such as base pairing, base stacking, and electrostatic repulsion of phosphate groups that give rise to the double-helical structure of the DNA with appropriate thermal and mechanical properties (26, 27). It gives a good account of the range of structural diversity of double-helical DNA (26). Details of the models can be found in *SI Appendix*.

The 3D structures predicted by our code compare well with the available crystal structures of $NF-\kappa B - DNA$. The tertiary and secondary levels of structure are reproduced in the simulations with high fidelity. The binding interface between protein and DNA is also well predicted. We also can compare the predicted complete structure of the complex $NF-\kappa B - I\kappa B$ with the crystal structure of an $NF-\kappa B - I\kappa B$ complex (PDB ID code 1IKN) in which the p50 binding domain has been removed (*SI Appendix*, Fig. S1). The crystal structure of the truncated complex aligns well with the simulated structure in the dimerization domain region. In the crystal structure of the truncated form, however, the p65 N-terminal binding domain has twisted further from its location in the $NF-\kappa B - DNA$ complex than it has in the predicted complete structure. This larger domain twist in the artificially truncated crystal structure results from the higher flexibility of the p65 N-terminal domain allowed by the absence of steric conflicts with the neighboring p50 N-terminal domain (*SI Appendix*, Fig. S1). When both N-terminal domains are present, the orientation of the domains is sterically forced to be closer to the orientation seen in the crystal structure of $NF-\kappa B - DNA$. Simulations of a heterodimer in which the p50 N-terminal binding domain has been removed concur in predicting this additional twist. In the following sections we make use of our predicted full structures of the bound complexes to follow their formation dynamics and reaction pathways.

Naturally occurring proteins are minimally frustrated as a result of evolutionary development. The ability of proteins to fold into unique native configurations on reasonable timescales is successfully explained by folding theories resting on the principle of minimal frustration (28–30). Frustration is not completely eliminated via evolutionary selection because functional constraints also sculpt the energy landscapes to allow functional motions of the folded proteins in the folded states and binding reactions (30, 31). The folded protein ensemble occupies the dominant basin of the free energy landscape where frustration properly localized in key regions of the protein chain opens up routes for specific functional dynamics.

Frustration in biomolecules can be readily quantified and visualized using a spatially local version of the principle of minimal frustration (30). An algorithm to do this is implemented in the frustratometer (32), which estimates the energetic contribution of contacts to the stability of the native state and compares these energies in the native structure to the distribution of energies that would be obtained by performing residue substitutions in the local environment. Native contacts whose energies are sufficiently deep in the energetically stabilizing part of the distribution are called

minimally frustrated and are drawn as green lines on the structure, whereas the native contacts that are found sufficiently far in the energetically destabilizing region are called frustrated and are drawn as red lines. The quantitative details of this algorithm including electrostatic effects have been discussed in previous papers (30, 32, 33).

The frustration patterns of the *NF- κ B* were analyzed in the structure of free *NF- κ B*, *NF- κ B* bound with the DNA, and *NF- κ B* bound with *I κ B*. When electrostatic effects are included, localized high levels of frustration are found in the binding pocket of the *NF- κ B* dimer when considered by itself (Fig. 2A) or when the protruding PEST sequence of the *I κ B* is truncated in the *NF- κ B* – *I κ B* dimer (Fig. 2B). This frustration is largely caused by the positively charged residues which are located in close proximity to each other. Binding DNA or the *I κ B* PEST sequence, both of which are negatively charged, mitigates this frustration so that the necklace of frustration in the binding pocket (Fig. 2A and B) becomes unfrustrated after DNA binds (Fig. 2C) or when the PEST sequence of the *I κ B* moves into the pocket (Fig. 2D). Thus, frustration analysis already hints that binding *I κ B* with its PEST can facilitate the stripping of *NF- κ B* from DNA by relieving frustration in the free *NF- κ B* that forms if the DNA dissociates by itself.

This origin of stripping is underlined by free energy calculations using umbrella sampling simulations of DNA binding to *NF- κ B* by itself and of DNA binding to a preexisting *I κ B* – *NF- κ B* complex. The starting structures for these simulations are the predicted structures previously described as well as a model of the ternary complex of *I κ B* – *NF- κ B* – DNA also created by AWSEM. From

these starting points we used umbrella sampling to sample more broadly the complete ensemble of conformational states intermediate between those where the partners are fully bound and other conformations where they are completely released. These simulations capture the steps of molecular stripping.

The distances between either the center of mass of the dimerization domains with the center of mass of the DNA or with the center of mass of the *I κ B* were used as harmonic biasing terms for the umbrella sampling. Whereas the in vitro experiments were carried out on the short piece of DNA that we used in simulations (SI Appendix, Fig. S2), we also carried out simulations that better mimic the way the transcription factor would approach a much longer full-length genomic DNA in vivo, by constraining the orientation of the DNA to remain parallel to the orientation of the initial bound state. Without this constraint an intermediate forms in which the protein complex binds to the apex of the short DNA fragment (SI Appendix, Fig. S3). Introducing the orientational constraint removes this artificial effect of the finite length of the DNA fragment studied in vitro.

The 1D free energy profiles for the biologically more relevant fixed orientation of the DNA (Fig. 3A) show that the binding of *I κ B* not only changes the DNA binding free energy to *NF- κ B* but also alters the detailed mechanism by which DNA associates with and dissociates from *NF- κ B*. *I κ B* lowers the barrier for DNA escape by at least 2–3 kcal (black arrows in Fig. 3A). This change implies that a considerable acceleration of the rate of dissociation from the DNA can be induced by binding *I κ B*. Looking at the profile from the DNA association viewpoint one sees that there is

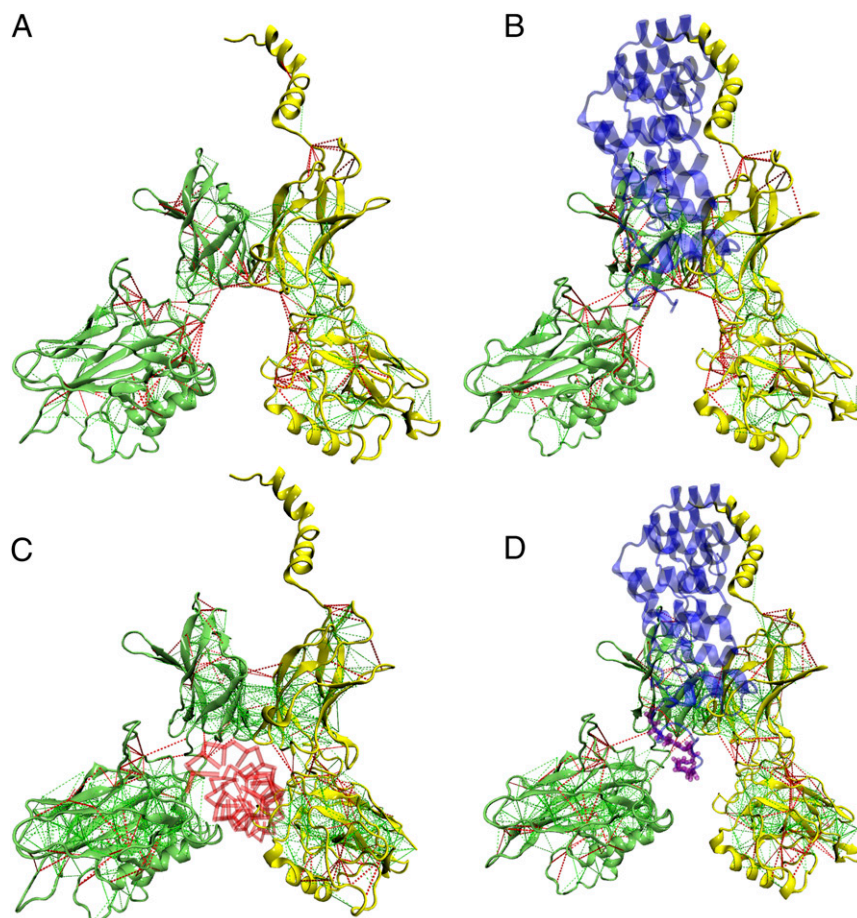


Fig. 2. Frustration analysis with electrostatics for the bound and free forms of the *NF- κ B*. Shown are the frustration patterns in (A) unbound *NF- κ B* dimer, (B) *NF- κ B* – *I κ B* complex with the PEST sequence removed, (C) *NF- κ B* – DNA complex, and (D) *NF- κ B* – *I κ B* complex.

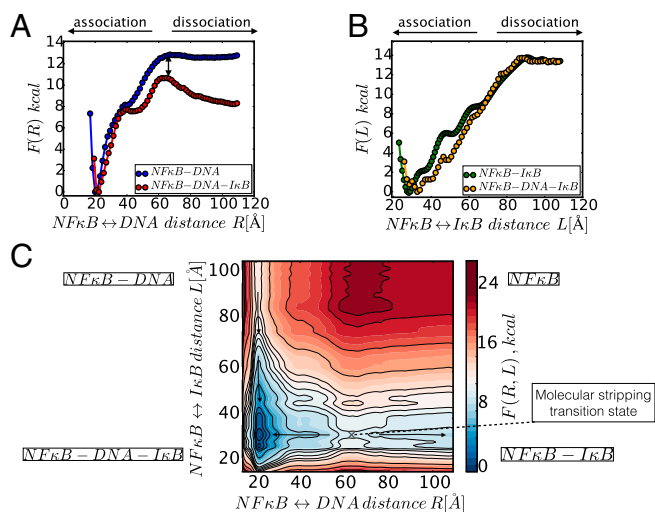


Fig. 3. (A) The 1D free energy profile for $I\kappa B$ dissociation from the ternary complex $I\kappa B - NF-\kappa B - DNA$. (B) The 1D free energy profile for DNA dissociation from the binary complex of $NF-\kappa B - DNA$ (in blue) and from the ternary complex of $I\kappa B - NF-\kappa B - DNA$ (in red). (C) A free energy surface combining the 1D plots in A and B. The initial, intermediate, and final configurations on a molecular stripping pathway can be seen in Fig. 6.

a significant kinetic barrier for DNA to associate with a preexisting $NF-\kappa B - I\kappa B$ complex, whereas DNA associates with free $NF-\kappa B$ in a diffusion-limited manner as shown by the purely downhill profile for binary association in the absence of $I\kappa B$.

Examining the free energy profile for $I\kappa B$ dissociation from the ternary complex (Fig. 3B) shows that there is a larger barrier for releasing $I\kappa B$ from the complex than for releasing DNA. This is in harmony with kinetic mixing experiments that do not observe dissociation of the $I\kappa B$ on the laboratory timescale (7, 12). Combining the two 1D free energy profiles into a 2D free energy surface (Fig. 3C) maps out the interchange of the two binding partners, through the approach of $I\kappa B$ to the binary complex with DNA and the subsequent dissociation of the DNA from the resulting ternary complex. Such a representation is reminiscent of the 20th-century pioneering studies of elementary gas phase reactions that made use of semiempirical surfaces (34) and quasi-classic mechanics (35) for obtaining detailed dynamical features of reactions. The dynamical and thermodynamic aspects of molecular stripping can be studied at a higher level of structural detail by using additional collective coordinates as discussed below. The lower barrier for DNA dissociation from the ternary complex $NF-\kappa B - DNA - I\kappa B$ compared with binary complex $NF-\kappa B - DNA$ and an even higher barrier for $I\kappa B$ dissociation (Fig. 3C) show that molecular stripping is not only thermodynamically but also kinetically favorable.

Essential Modes of Motion

Being a multidomain protein complex, as expected, the $NF-\kappa B$ heterodimer can bend around the connecting hinge while the individual domains themselves remain relatively rigid. To characterize this and other global slow timescale motions we performed many exhaustive simulations with a cumulative run time equivalent to more than 500 μs of real time. The long sampling times are made possible by using our coarse-grained model. Using long constant temperature simulations we first carried out principal component analysis in the Cartesian space spanned by the backbone C_α atoms of the free $NF-\kappa B$ alone to uncover the dominant large amplitude modes of motion. Principal component analysis of well-sampled trajectories of proteins in their native states provides a convenient simplifying lens to characterize their functional collective motions (31, 36).

The first principal component is the predominant motion that accounts for more than 70% of the amplitude of motion in unbound $NF-\kappa B$ (SI Appendix, Fig. S4), but a second component also plays a role. Projection of the equilibrium ensemble of structures onto these two modes reveals that these large-amplitude motions are not quasi-harmonic in the free $NF-\kappa B$ dimers, leading to multipik distributions for these collective coordinates in the free form (Fig. 4A and SI Appendix, Fig. S5). The first principal component is largely a domain twist motion (SI Appendix, Fig. S6 and Movie S1). The second principal component for the free $NF-\kappa B$ is an overall domain breathing motion, resembling the opening and closing of the DNA binding cavity (SI Appendix, Fig. S6 and Movie S2). In contrast to the free $NF-\kappa B$ case, for both binary complexes the distribution of these coordinates is essentially single-peaked, with peaks in different locations for $NF-\kappa B - I\kappa B$ and for $NF-\kappa B - DNA$ (Fig. 4A). $I\kappa B$ binding and DNA binding couple to distinct motions of the free $NF-\kappa B$, namely dominantly to the twist when forming $I\kappa B - NF-\kappa B$ but to the breathing mode when forming $NF-\kappa B - DNA$.

Projecting the equilibrium ensemble of the binary complexes on principal components determined now by including both backbone atoms of $NF-\kappa B$ and the backbone atoms of its binding partners (either DNA or $I\kappa B$) reveals the motions of the partners with respect to each other. The principal motion of the $NF\kappa B - DNA$ complex corresponds to sliding the $NF-\kappa B$ along the DNA strands (SI Appendix, Fig. S6), supporting the view that $NF-\kappa B$ can easily perform a 1D diffusional motion along the DNA without being released. The second largest principal component for $NF-\kappa B - DNA$ as a whole complex corresponds to what was the domain twist motion of the free $NF-\kappa B$. The domain breathing motion that is displaced upon DNA binding is heavily suppressed in fluctuating amplitude after the DNA binds.

When $I\kappa B$ binds to free $NF-\kappa B$ the induced twist orients the domains so that only one of the $NF-\kappa B$ monomers can now contact the DNA very closely (Fig. 4B). This observation is one of the key results of this work. We see that $I\kappa B$ acts as an allosteric effector precisely by selecting a conformation in the $NF-\kappa B - DNA$ most favorable for DNA dissociation. Once the $I\kappa B$ binds the $NF-\kappa B$, the DNA remains held by only a single N-terminal domain of $NF-\kappa B$ coming from the p50 subunit (Fig. 4B). In contrast, both N-terminal domains contribute to holding strongly to the DNA before the twist transition has taken place. The allosteric change through twisting ultimately allows the stripping of $NF-\kappa B$ from its genomic binding sites on the DNA.

Mechanistic Picture of Molecular Stripping

By mapping the free energy profile simultaneously onto the dissociation distances (Fig. 3) and onto the principal components

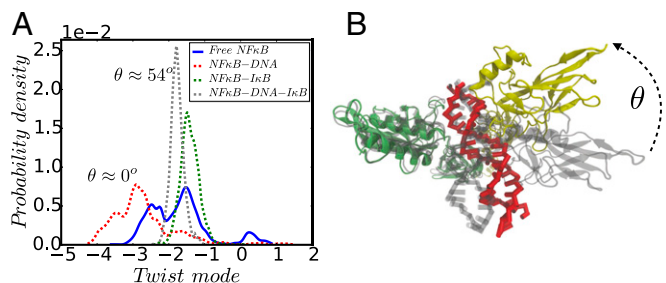


Fig. 4. (A) Distribution of conformational ensembles for free and bound forms of $NF-\kappa B$ along the twist mode coordinate of free $NF-\kappa B$. (B) The p50 domain of the binary complex (gray) was aligned with the p50 domain of the ternary $NF-\kappa B - DNA - I\kappa B$ complex (p50, green; p65, yellow; DNA, red; $I\kappa B$, not shown). The $I\kappa B$ induces a twist in the relative orientation of the p50 and p65 domains (angle θ).

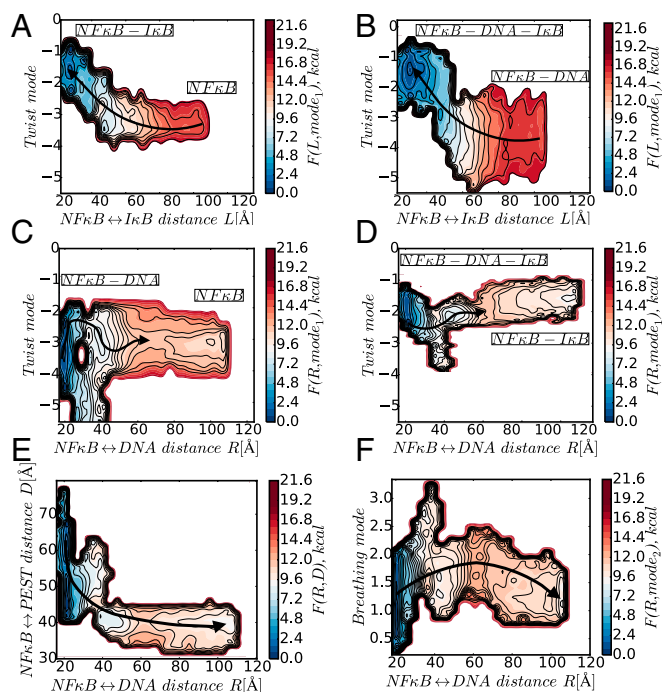


Fig. 5. (A–D) Free energy surfaces mapped onto relevant dissociation/association distances and the domain twist mode. Dark arrows indicate the direction of the most favorable path leading to formation of stable complexes. (A) Free energy surface for $NF-\kappa B$ binding to $I\kappa B$ forming a binary complex $I\kappa B - NF-\kappa B$. (B) Free energy surface for $NF-\kappa B - DNA$ binding to $I\kappa B$ forming a ternary complex $NF-\kappa B - DNA - I\kappa B$. (C) Free energy surface for DNA dissociation from the binary complex $NF-\kappa B - DNA$ to form free $NF-\kappa B$. (D) Free energy surface for DNA dissociation from the ternary complex $NF-\kappa B - DNA - I\kappa B$ to form the binary complex $NF-\kappa B - I\kappa B$. (E) Free energy surface mapped onto the DNA dissociation distance and the PEST distance from the binding pocket of the $NF-\kappa B$ in the ternary complex of the $NF-\kappa B - DNA - I\kappa B$. (F) Free energy for dissociation of the $DNA - NF-\kappa B$ complex mapped onto the DNA dissociation distance and onto the breathing mode that opens and closes the DNA binding cavity.

of free $NF-\kappa B$ we can uncover the key mechanistic steps by which DNA dissociates from $NF-\kappa B$ after the complex with $I\kappa B$ forms. Following how the domain twist coordinate changes as the partners approach each other we see that the minimal free energy paths for dissociation of DNA have two stages (Fig. 5). In

the first stage the domains twist (note the solid arrows in Fig. 5A and B), thereby loosening the steric and electrostatic grip of the transcription factor on the DNA. This twist is then followed by a subsequent step in which the DNA separates from the complex whereas only one of the two domains holds on strongly to the DNA. The free energy surface for DNA dissociation from the binary complex $NF-\kappa B - DNA$ (Fig. 5C) shows a bifurcation: The DNA can be induced to dissociate by rotating either of the two DNA binding domains. The two dissociating paths do not have equal barriers, which highlights the symmetry breaking in the heterodimer of $NF-\kappa B$.

Dissociation of DNA from the ternary complex proceeds by a different route (Figs. 5D and 6) than does DNA dissociation from the binary complex because the binding of the $I\kappa B$ to the $NF-\kappa B - DNA$ binary complex has already induced the necessary domain twist of the p65 domain via a conformational selection mechanism (Fig. 5B). In forming the ternary complex the DNA binding domain has already come to a more favorable orientation for releasing DNA, leading to lower kinetic barriers (Fig. 5D). We see the first step of molecular stripping occurs through an allosteric transition caused by the $I\kappa B$ acting on the domain twist mode of the $NF-\kappa B$ heterodimer. This conformational change facilitates the stripping of the $NF-\kappa B$ from DNA by decreasing the barrier for further domain twist. Once DNA leaves the ternary intermediate, the resulting bound complex of $NF-\kappa B - I\kappa B$ is thermodynamically much more stable (Fig. 5A) than the starting complex with $NF-\kappa B$ bound only to the DNA (Fig. 5B). It is then no surprise that the reverse reaction of DNA stripping the $I\kappa B$ moiety from its complex with $NF-\kappa B$ has not been observed in kinetic experiments (7). The thermodynamic stability of the $NF-\kappa B - I\kappa B$ complex as well as the origin of barrier for the reverse reaction of DNA binding can be explained using electrostatic arguments as follows. In the second step of stripping, as the DNA begins to leave, the $I\kappa B$ reconfigures through the motion of the PEST sequence. By being highly negatively charged the PEST sequence begins to compete with the DNA for binding to the positively charged $NF-\kappa B$ binding pocket (Fig. 5E). This exchange of partners lowers the barrier for DNA dissociation.

As is seen on the free energy surface, once the DNA has completely left the cavity, the PEST sequence moves still further to occupy the cavity, thereby finally resolving the electrostatically frustrated interactions (Figs. 5E and 6). Looked at hypothetically in the reverse direction of association, the occupation of the DNA binding pocket by the PEST sequence leads to a free energy barrier inhibiting association of the DNA with the $NF-\kappa B - I\kappa B$ complex. This barrier gives another way by which $I\kappa B$ controls the

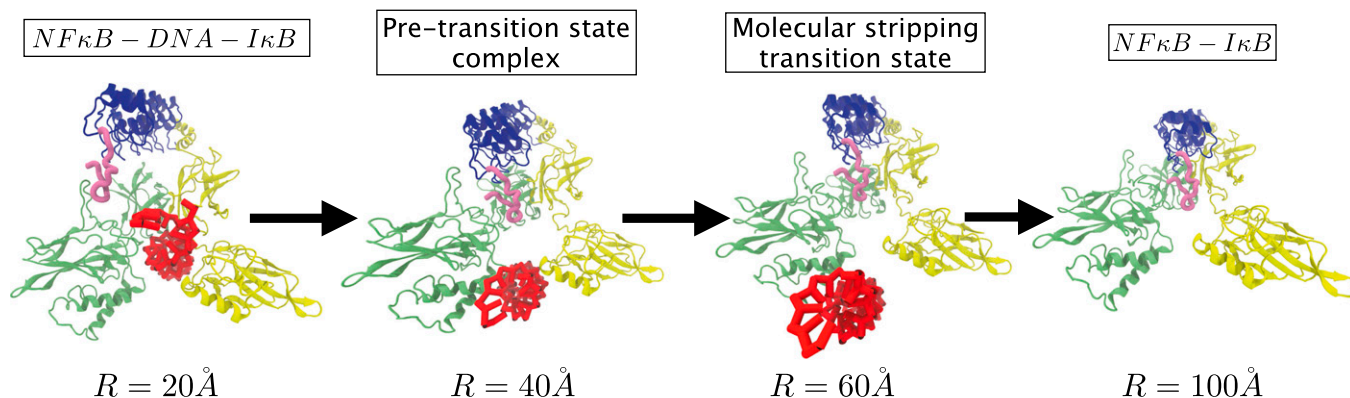


Fig. 6. The progression of structural changes on the molecular stripping path starting from the ternary complex $DNA - NF-\kappa B - I\kappa B$ and going through the states of the pretransition state complex, the molecular stripping transition state, and ending at the stable binary complex of $I\kappa B - NF-\kappa B$. The pink tube highlight shows the PEST sequence and its motion with respect to the $NF-\kappa B$ throughout the DNA dissociation. The partial collapse of the binding cavity once the DNA has left is also evident.

transcriptional ability of the *NF-κB*. Note that in both the pre-transition state complex and the molecular stripping transition state itself the DNA remains bound transiently to the p50 subunit for which it has the higher affinity (37).

One may use other collective modes for investigating different mechanistic aspects of *NF-κB* domain motions. For instance, using the breathing mode as a collective coordinate (Fig. 5F) reveals a displacement in the breathing mode coordinate when DNA dissociates or binds to the free *NF-κB*. The two DNA binding domains of *NF-κB* first open and then close, approaching each other to seal the cavity between them, thus locking onto the target DNA.

Materials and Methods

A detailed description of the materials and methods is given in *SI Appendix, Materials and Methods*. Briefly, the simulations were carried out using electrostatically enhanced version of AWSEM force field for proteins (33) and 3SPN2c force field for DNA (22, 23). All simulations were done under constant temperature conditions, following the standard protocols of minimization and equilibration starting from either computationally predicted or available crystal structures. Principal component analysis was performed on an ensemble of structures generated by carrying out multiple independent constant temperature simulations with a cumulative time equivalent to over 500 μs of real time. Close to 100 large-scale domain change events have been registered in the simulations, each of which is estimated to take place on a 1- to 10-μs timescale. Free energy profiles were computed by carrying out umbrella sampling by restraining protein-protein and protein-DNA center of mass distances with harmonic constraints.

- Ptashne M (1986) Gene regulation by proteins acting nearby and at a distance. *Nature* 322(6081):697–701.
- Ptashne M (2004) *A Genetic Switch: Phage Lambda Revisited* (Cold Spring Harbor Lab Press, Cold Spring Harbor, NY), Vol 3.
- Gilbert W, Müller-Hill B (1966) Isolation of the lac repressor. *Proc Natl Acad Sci USA* 56(6):1891–1898.
- Jacob F, Monod J (1961) Genetic regulatory mechanisms in the synthesis of proteins. *J Mol Biol* 3:318–356.
- Ackers GK, Johnson AD, Shea MA (1982) Quantitative model for gene regulation by lambda phage repressor. *Proc Natl Acad Sci USA* 79(4):1129–1133.
- Phillips R, Kondev J, Theriot J, Garcia H (2012) *Physical Biology of the Cell* (Garland, New York).
- Alverdi V, Hetrick B, Joseph S, Komives EA (2014) Direct observation of a transient ternary complex during IκBα-mediated dissociation of NF-κB from DNA. *Proc Natl Acad Sci USA* 111(11):225–230.
- Oeckinghaus A, Ghosh S (2009) The NF-kappaB family of transcription factors and its regulation. *Cold Spring Harb Perspect Biol* 1(4):a000034.
- Krappmann D, et al. (2004) The IκappaB kinase complex and NF-kappaB act as master regulators of lipopolysaccharide-induced gene expression and control subordinate activation of AP-1. *Mol Cell Biol* 24(14):6488–6500.
- Hoffmann A, Levchenko A, Scott ML, Baltimore D (2002) The IκappaB-NF-kappaB signaling module: Temporal control and selective gene activation. *Science* 298(5596):1241–1245.
- Nelson DE, et al. (2004) Oscillations in NF-kappaB signaling control the dynamics of gene expression. *Science* 306(5696):704–708.
- Bergqvist S, et al. (2006) Thermodynamics reveal that helix four in the NLS of NF-kappaB p65 anchors IκappaBα, forming a very stable complex. *J Mol Biol* 360(2):421–434.
- Baeuerle PA, Baltimore D (1988) I kappa B: A specific inhibitor of the NF-kappa B transcription factor. *Science* 242(4878):540–546.
- Jacobs MD, Harrison SC (1998) Structure of an IκappaBα/NF-kappaB complex. *Cell* 95(6):749–758.
- Williams RA, Timmis J, Qvarnstrom EE (2014) Computational models of the NF-KB signalling pathway. *Computation* 2(4):131–158.
- Cheong R, Hoffmann A, Levchenko A (2008) Understanding NF-kappaB signaling via mathematical modeling. *Mol Syst Biol* 4:192.
- Bergqvist S, et al. (2009) Kinetic enhancement of NF-kappaBxDNA dissociation by IκappaBα. *Proc Natl Acad Sci USA* 106(46):19328–19333.
- Martone R, et al. (2003) Distribution of NF-kappaB-binding sites across human chromosome 22. *Proc Natl Acad Sci USA* 100(21):12247–12252.
- Berkowitz B, Huang DB, Chen-Park FE, Sigler PB, Ghosh G (2002) The x-ray crystal structure of the NF-κ B p50.p65 heterodimer bound to the interferon β -κ B site. *J Biol Chem* 277(27):24694–24700.
- Huxford T, Huang DB, Malek S, Ghosh G (1998) The crystal structure of the IκappaBα/NF-kappaB complex reveals mechanisms of NF-kappaB inactivation. *Cell* 95(6):759–770.
- Davtyan A, et al. (2012) AWSEM-MD: Protein structure prediction using coarse-grained physical potentials and bioinformatically based local structure biasing. *J Phys Chem B* 116(29):8494–8503.
- Hinckley DM, Freeman GS, Whitmer JK, de Pablo JJ (2013) An experimentally-informed coarse-grained 3-Site-Per-Nucleotide model of DNA: Structure, thermodynamics, and dynamics of hybridization. *J Chem Phys* 139(14):144903.
- Freeman GS, Hinckley DM, Lequieu JP, Whitmer JK, de Pablo JJ (2014) Coarse-grained modeling of DNA curvature. *J Chem Phys* 141(16):165103.
- Onuchic JN, Luthey-Schulten Z, Wolynes PG (1997) Theory of protein folding: The energy landscape perspective. *Annu Rev Phys Chem* 48:545–600.
- Zheng W, Schafer NP, Davtyan A, Papoian GA, Wolynes PG (2012) Predictive energy landscapes for protein-protein association. *Proc Natl Acad Sci USA* 109(47):19244–19249.
- Potoyan DA, Savelyev A, Papoian GA (2013) Recent successes in coarse-grained modeling of DNA. *WIREs Comp Mol Sci* 3:69.
- de Pablo JJ (2011) Coarse-grained simulations of macromolecules: From DNA to nanocomposites. *Annu Rev Phys Chem* 62:555–574.
- Bryngelson JD, Wolynes PG (1987) Spin glasses and the statistical mechanics of protein folding. *Proc Natl Acad Sci USA* 84(21):7524–7528.
- Bryngelson JD, Onuchic JN, Socci ND, Wolynes PG (1995) Funnels, pathways, and the energy landscape of protein folding: A synthesis. *Proteins* 21(3):167–195.
- Ferreiro DU, Komives EA, Wolynes PG (2014) Frustration in biomolecules. *Q Rev Biophys* 47(4):285–363.
- Zhuravlev PI, Papoian GA (2010) Protein functional landscapes, dynamics, allostery: A tortuous path towards a universal theoretical framework. *Q Rev Biophys* 43(3):295–332.
- Jenik M, et al. (2012) Protein frustratometer: A tool to localize energetic frustration in protein molecules. *Nucleic Acids Res* 44:71.
- Tsai MY, et al. (August 8, 2015) Electrostatics, structure prediction, and the energy landscapes for protein folding and binding. *Protein Sci*, 10.1002/pro.2751.
- Eyring H, Polanyi M (1931) Uber einfache gasreaktionen. *Z Phys Chem Abt B* 12:279.
- Hirschfelder J, Eyring H, Topley B (1936) Reactions involving hydrogen molecules and atoms. *J Chem Phys* 4:170.
- Potoyan DA, Papoian GA (2011) Energy landscape analyses of disordered histone tails reveal special organization of their conformational dynamics. *J Am Chem Soc* 133(19):7405–7415.
- Phelps CB, Sengchanthalangsy LL, Malek S, Ghosh G (2000) Mechanism of κ B DNA binding by Rel/NF-κ B dimers. *J Biol Chem* 275(32):24392–24399.

Concluding Remarks

Single-cell experiments on *NF-κB* regulation in vivo, mathematical modeling, in vitro kinetics, and structural studies have provided many important clues to *NF-κB* signaling systems biology. The present simulations show that a detailed molecular-level understanding of the functional dynamics of the key *NF-κB* – *IκB* – DNA genetic switch elements can add more to the story. In this work exhaustive long timescale, coarse-grained simulations for the free *NF-κB* heterodimer and its bound complexes with DNA and *IκB* have allowed us to explore structures, thermodynamics, and motions that have not been accessible to direct crystallographic study. Our simulations demonstrate that the *NF-κB*/DNA/*IκB* switch functions via an allosteric mechanism that involves conformational selection of a collective mode of domain twist accompanied by opening and closing of the cavity between the two DNA binding domains of the heterodimer. The molecular stripping process of *NF-κB* from its target genetic sites by *IκB* proves both kinetically and thermodynamically favorable, suggesting a novel nonequilibrium mechanism for the efficient control of gene expression in this important master regulator system.

ACKNOWLEDGMENTS. We thank Holly Dembinsky, Kristen Ramsey, Bin Zhang, and Patricio Craig for numerous stimulating discussions. This work was supported by PPG Grant P01 GM071862 from the National Institute of General Medical Sciences. This work was also supported by the D. R. Bullard-Welch Chair at Rice University, Grant C-0016 (to P.G.W.).